

# Metal-Film-Coated Silica Nanoparticle Monolayers for Application in Surface Enhanced Raman Scattering

Nguyen Thi Thanh Lan<sup>1</sup>, Nguyen Thi Hai Yen<sup>1,2</sup>,  
Luu Thi Lan Anh<sup>2</sup>, Chu Manh Hoang<sup>1\*</sup>

<sup>1</sup>International Training Institute for Materials Science,  
Hanoi University of Science and Technology, Hanoi, Vietnam

<sup>2</sup>School of Engineering Physics, Hanoi University of Science and Technology, Hanoi, Vietnam

\*Corresponding author email: hoangcm@itims.edu.vn

## Abstract

Surface enhanced raman scattering is interested for a variety of applications, especially in determining the presence of substances at very low concentrations, at the level of ppm, that is obtained by amplifying the raman scattering signal of adsorbent particles on metal surfaces or nanostructures. In this paper, we report on surface enhanced raman scattering substrates based on metal-film-coated silica nanoparticle monolayer. The silica nanoparticles having the diameter of 196 nm are assembled into close-packaged monolayer on silicon substrate by spin coating technique. The gap among the silica nanoparticles is tuned by HF vapor etching. The investigations on reflectance characteristic and raman spectra show that close- and non-close-packaged monolayers on silicon substrate covered by a thin gold layer can be used as surface enhanced raman scattering substrates.

Keywords: Silica nanoparticle, spin coating, self-assembled nanoparticle monolayer, surface-enhanced raman scattering

## 1. Introduction

Surface-enhanced Raman Scattering (SERS) is a measurement technique that determines the presence of substances at very low concentrations. SERS substrates are used to detect low levels of biological molecules and thus can detect proteins in bodily fluids [1]. This technology has been used to detect urea in human serum and could become the next generation of technology in cancer screening and detection [2]. The sensitivity is enhanced by amplifying the raman scattering signal of adsorbent particles on metal surfaces or nanostructures such as plasmonic silica nanotubes [3]. Raman scattering enhancement coefficients can reach  $10^{10}$  to  $10^{11}$ , even this technique can be used to detect monomolecules [4].

Although SERS can be performed in colloidal solutions, currently the most common method for performing SERS measurements is to deposit a liquid sample onto a silicon or glass surface with a nanostructured metal surface. The SERS tests can be performed on silver surfaces formed by electrochemical method, covered with metal nanoparticles [5], etching method [6] or porous silicon as the support material for patterning nanostructures [5,7]. Silver metal-coated silicon nanotubes were also used to create the SERS substrate [8]. For applications

in practice, fabrication costs of SERS substrates should be minimized and highly sensitive SERS substrates have been studied extensively [9-11]. The low cost, effective method for producing SERS substrates is currently based on lithography using assembled silica nanoparticle monolayer. The obtained results can name a few such as nanomachining by colloidal lithography, the photolithography-assisted process for the fabrication of periodic nanoarrays, or the construction of colorimetric sensors for gas, chemical, and biomedical detection [12-14]. Especially, the recent approaches in fabricating non-close silica nanoparticle monolayer using drop-coating and HF vapor etching is reported in [15,16], the gap among silica nanoparticles having the size of 50 nm in the monolayer can be tuned at nanoscale.

The paper presents the results obtained from investigations of close- and non-close-packaged monolayers on silicon substrate covered by thin gold layer as SERS substrates. Raman scattering spectra of methylene blue (MB) on SERS substrates is experimentally investigated.

## 2. Experiment

To fabricate spherical silica nanoparticles, we have used Stober method. Tetraethylorthosilicate (TEOS) is the precursor, while ethanol solvent, water, and ammonia are the agent and catalyst for hydrolysis

reaction [17,18]. The concentration and volume of the solutions are as follows:  $C_2H_5OH$  (50 ml),  $NH_3$  2M (7.8 ml), TEOS 0.3M (5.34 ml). With the ratio of catalyst as above specified, the concentration of  $H_2O$  in ammonia solution is determined at about 5M. The process for synthesizing spherical silica nanoparticles is carried out by slowly adding the first solution containing the mixture of TEOS and  $C_2H_5OH$  to the second solution containing  $C_2H_5OH$  and  $NH_3$ . The final solution is magnetically stirred at room temperature until silica nanoparticles are formed, then silica nanoparticles are centrifuged and repeatedly washed with ethanol until  $pH \approx 7$ . The silica nanoparticles are dispersed in ethanol and stored at low temperature. Synthesized nanoparticles were characterized by field emission scanning electron microscope (FE-SEM) with Hitachi's S-4800 FE-SEM.

In this study, we have fabricated silica nanoparticle monolayers on silicon substrates having the dimensions of  $1\text{ cm} \times 1\text{ cm}$ . The silicon substrate is cleaned by ultrasonic vibration in acetone, ethanol, and deionized water. The Si substrate is immersed in piranha solution (the volume ratio  $H_2SO_4$  (98%) :  $H_2O_2$  (35%) = 3 : 1) for 18 h at room temperature and rinsing with deionized water, which is used for increasing adhesion between silica nanoparticles and the surface of the substrate [15,16]. The silica nanoparticle monolayers are then assembled on the silicon substrate by the one-step spin-coating technique under ambient temperature condition of  $25\text{ }^\circ\text{C}$  and relative humidity of 65% for 150 s at spin-coating speed of 2000 rpm. The annealing process is carried out at  $800\text{ }^\circ\text{C}$  for 30 min. to enhance the adhesion of silica nanoparticles assembled on silicon substrates. The annealed close-packaged silica nanoparticle monolayers are then etched in HF vapour for decreasing the size, resulting in non-close-packaged monolayers. Some samples were annealed the second time at  $950\text{ }^\circ\text{C}$  for 30 min to enhance the adhesion of silica nanoparticles after the first etching process. A 20 nm Au thin film layer is sputter deposited on the silica nanoparticle monolayers to form plasmonic substrates.

### 3. Results and Discussions

Fig. 1 shows FESEM images of the close-packaged silica monolayer assembled by spin coating technique before etched in HF vapor and sputtered a metal layer for forming the plasmonic substrate. Thus, the synthesized silica nanoparticles are quite homogeneous; their average size is determined to be 196 nm with a standard deviation approximately  $\pm 40\text{ nm}$ . Fig. 2 shows FESEM images of silica nanoparticle monolayers, before (a) and after (b) etched in HF vapor for 100 s, coated with a 20 nm gold metal film layer.

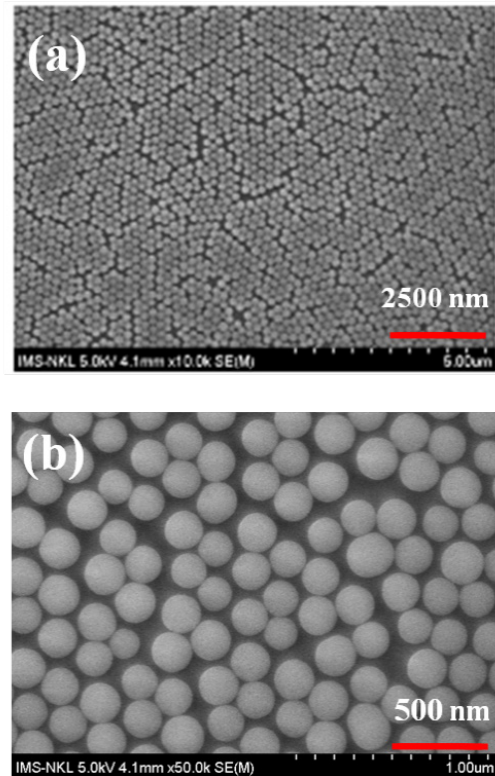


Fig. 1. FESEM images of close-packaged silica monolayer assembled by spin coating technique: (a) a total view and (b) a close view.

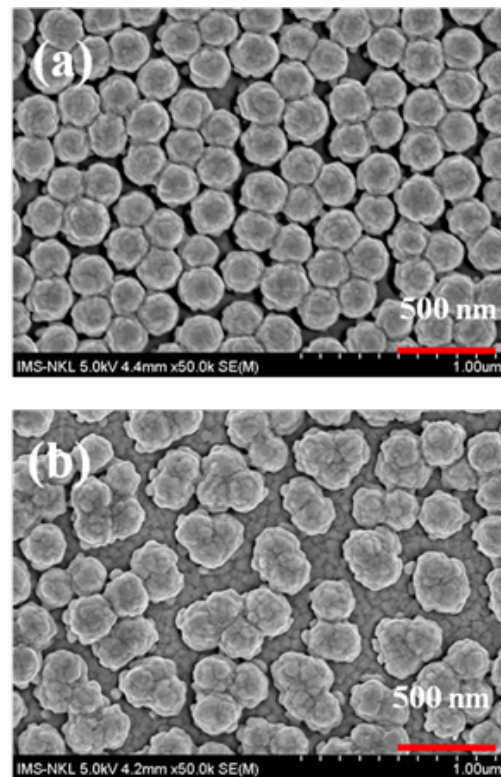


Fig. 2. FESEM image of silica nanoparticle monolayer coated with a thin gold metal film layer: (a) non-etched silica nanoparticles and (b) silica nanoparticles etched in HF vapor for 100 s.

Fig. 3 shows reflectance spectrum of non-etched and etched silica nanoparticle monolayer samples sputtered a 20 nm Au layer. Gold metal absorbs significantly light at wavelengths below 550 nm due to two interband transitions at wavelengths of 330 nm and 470 nm. The wavelength regions have capability of plasmonic resonances to be above the strong absorption region and the resonance modes are excited at wavelengths larger than 500 nm. Due to the rough surface, the reflectivity of gold on the nanostructured substrate is reduced compared to that on the flat glass substrate. The samples are not etched and etched for 100 s having a clear resonance peak in the visible region (concave region on the reflectance spectrum), at wavelengths  $\sim 540$  nm and  $\sim 610$  nm, respectively. Red shift resonance and reflection decrease stronger when the etching time increases to 130 s, because the HF vapor reacts with the silica nanoparticles to create products containing water, so etched silica nanoparticles tend to aggregate together, increasing size and changing the shape of initial plasmonic nanoparticles. Consequently, the gap between nanoparticles also increases (Fig. 2b).

Plasmon resonance properties of silica nanoparticle monolayer coated gold metal were investigated by raman scattering spectrum on a  $\mu$ -Raman equipment (Renishaw in Via micro-Raman). The condition for an enhanced raman scattering effect is that the exciting laser wavelength is in the resonance region of the plasmonic substrate, the absorption and scattering produce photons with energies different from the incident photons. The effect is increased if the photon scattering is also capable of stimulating plasmon resonance [19,20].

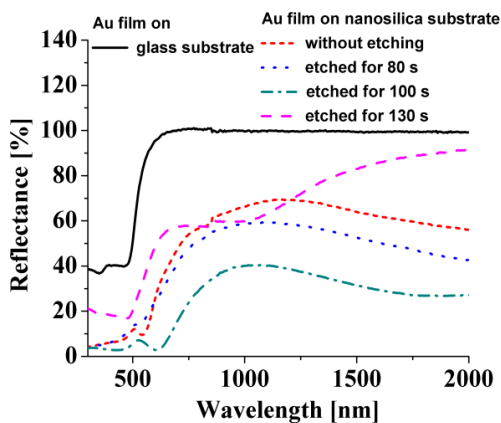


Fig. 3. Reflective spectrum of a 20 nm Au film sputtered deposited on glass substrate and non-etched and etched silica nanoparticle monolayers.

Using an excitation laser at wavelength  $\lambda = 633$  nm and the counting time of 30 s, Fig. 4a shows that for the substrate having monolayer of silica nanoparticles there is only the appearance of a raman scattering peak corresponding to the high order oscillation of Si around  $940-970$   $\text{cm}^{-1}$  [21]. When

coated with a gold layer, this peak is no longer shown because it is blocked by the metal layer, while the peak relating to Si-O bonding of silica nanoparticles ( $\sim 990$   $\text{cm}^{-1}$ ) is enhanced by localized plasmon resonance around the core-shell structured nanoparticles (Fig. 4b).

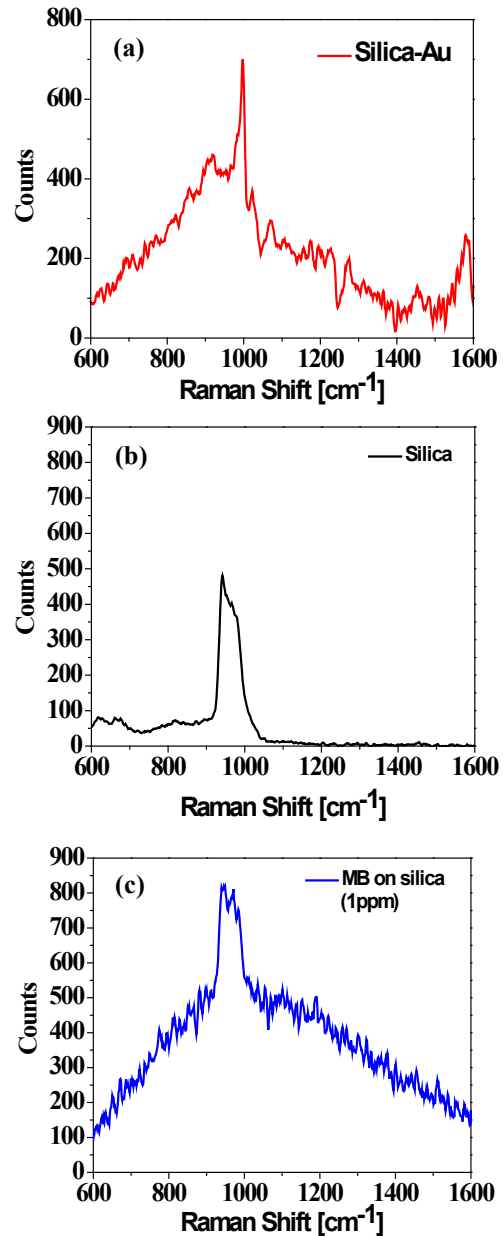


Fig. 4. Raman scattering spectra of (a) Si substrate having close-packaged silica nanoparticle monolayer, (b) Si substrate having close-packaged silica nanoparticle monolayer sputtered with a 20 nm gold film layer, and (c) Si substrate having close-packaged silica nanoparticle monolayer after adsorbing MB (1 ppm).

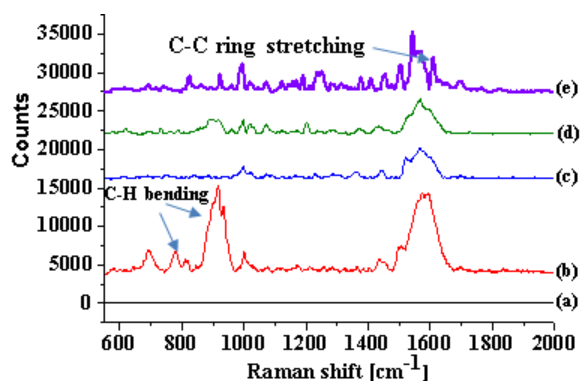


Fig. 5. Raman scattering spectra of MB deposited on different substrates: (a) Si substrate having close-packed silica nanoparticle monolayer deposited MB with a concentration of 1 ppm; (b) gold-coated non-etched silica nanoparticle monolayer substrate, (c) and (d) gold-coated silica nanoparticle monolayer substrates with etching times of silica nanoparticles in HF vapor to be 80 s and 100 s, respectively, and (e) gold-coated silica nanoparticle monolayer substrate after etched for 100 s and annealed at 950 °C and deposited MB with a concentration of 1 ppm.

Fig. 4c and Fig. 5 show the raman scattering spectra of the dried substrates after dropping a drop of MB with volume of 7-10  $\mu\text{L}$  at a concentration of  $10^{-6}$  M (Fig. 4c and 5a) and  $10^{-9}$  M (Fig. 5b-5e), the photon counting time is 10 s. The results of measuring raman scattering in the wavenumber range 550-2000  $\text{cm}^{-1}$  show that on the substrate without plasmonic metal (Fig. 4c and 5a), the scattering peaks of MB molecules are almost not shown. The substrates containing gold-coated silica nanoparticles (Fig. 5b-5e) have localized plasmon resonance, so the raman scattering peak of MB molecule is enhanced, however, they are not the same, some characteristic peaks appear at 770  $\text{cm}^{-1}$ , 900  $\text{cm}^{-1}$ , 1184  $\text{cm}^{-1}$ , and 1620  $\text{cm}^{-1}$ , corresponding to the fluctuation of bonds C-H and C-C in the MB molecule [22]. Furthermore, to represent for the sensitivity of a SERS substrate, one often uses the SERS enhancement factor  $EF$ , which is defined by  $EF = (I_{SERS} / I_{norm}) \cdot (N_{norm} / N_{SERS})$ , where  $I_{SERS}$  is the intensity of SERS signal,  $I_{norm}$  is the average raman intensity,  $N_{norm}$  is the average number of molecules in the scattering volume for the raman (non-SERS) measurement, and  $N_{SERS}$  is the average number of adsorbed molecules in the scattering volume for the SERS experiments [23]. However, in this study, we only focus on examining the ability of sensing MB molecule with low concentration. To determine the  $EF$  value, the comprehensive investigations need to be carried out, which will be reported in other work. Thus, coating metal on silica nanoparticle monolayer substrates is also an effective method to obtain a uniform plasmonic substrate, for applications in detecting organic matters with small concentrations.

#### 4. Conclusion

In summary, we have presented the results of investigating surface enhanced raman scattering substrate based on metal-film-coated 196 nm silica nanoparticle monolayer. The silica nanoparticle monolayers in close- and non-close-packaged types have been obtained by spin coating technique and HF vapor etching. These monolayers are sputtered with a 20 nm Au layer and then used as surface enhanced raman scattering substrates in determining methylene blue concentration at the level of  $10^{-6}$  M and  $10^{-9}$  M. The Raman scattering spectra of methylene blue on silica monolayer substrates with and without thin gold film shows the enhancement of spectra due to localized plasmon resonance formed by metal-film-coated silica nanoparticles.

#### Acknowledgments

This work is funded by the Hanoi University of Science and Technology (HUST) under project number T2020-SAHEP-024.

#### References

- [1] N. Banaei *et al.*, Multiplex detection of pancreatic cancer biomarkers using a SERS-based immunoassay, *Nanotechnology*, vol. 28, no. 45, Sept. 2017, Art. no. 455101. <https://doi.org/10.1088/1361-6528/aa8e8c>
- [2] Y. A. Han, J. Ju, Y. Yoon, S. M. Kim, Fabrication of cost-effective surface enhanced Raman spectroscopy substrate using glancing angle deposition for the detection of urea in body fluid, *J. Nanosci. Nanotechnol.*, vol. 14, no. 5, pp. 3797-3799, May 2014. <https://doi.org/10.1166/jnn.2014.8184>
- [3] X. Xu, H. Li, D. Hasan, R. S. Ruoff, A. X. Wang, and D. L. Fan, Near-field enhanced plasmonic-magnetic bifunctional nanotubes for single cell bioanalysis, *Adv. Funct. Mater.*, 2013. <https://doi.org/10.1002/adfm.201203822>
- [4] E. J. Blackie, E. C. L. Ru., P. G. Etchegoin, Single-molecule surface-enhanced raman spectroscopy of nonresonant molecules, *J. Am. Chem. Soc.*, vol. 131, no. 40, pp. 14466-14472, 2009. <https://doi.org/10.1021/ja905319w>
- [5] J. J. Mock, M. Barbic, D. R. Smith, D. A. Schultz, and S. Schultz, Shape effects in plasmon resonance of individual colloidal silver nanoparticles, *J. Chem. Phys.*, vol. 116, no. 15, 2002, Art. no. 6755. <https://doi.org/10.1063/1.1462610>
- [6] E. H. Witlicki *et al.*, Molecular logic gates using surface-enhanced raman-scattered light, *J. Am. Chem. Soc.*, vol. 133, no. 19, pp. 7288-7291, 2011. <https://doi.org/10.1021/ja200992x>
- [7] H. Lin, J. Mock, D. Smith, T. Gao, and M. J. Sailor, Surface-enhanced raman scattering from silver-plated porous silicon, *J. Phys. Chem. B.*, vol. 108, no. 31, pp. 11654-11659, Aug. 2004. <https://doi.org/10.1021/jp049008b>

- [8] K. N. Kanipe, P. P. F. Chidester, G. D. Stucky, and M. Moskovits, Large format surface-enhanced raman spectroscopy substrate optimized for enhancement and uniformity, *ACS Nano*, vol. 10, no. 8, pp. 7566-7571, 2016.  
<https://doi.org/10.1021/acsnano.6b02564>
- [9] C. H. Lee, L. Tian, and S. Singamaneni, Paper-based SERS, *ACS Appl. Mater. Interfaces*, vol. 2, no. 12, pp. 3429-3435, 2010.  
<https://doi.org/10.1021/am1009875>
- [10] J. J. Laserna, A. D. Campiglia, and J. D. Winefordner, Mixture analysis and quantitative determination of nitrogen-containing organic molecules by surface-enhanced Raman spectrometry, *Anal. Chem.*, vol. 61, no. 15, pp. 1697-1701, 1989.  
<https://doi.org/10.1021/ac00190a022>
- [11] W. W. Yu and I. M. White, Inkjet-printed paper-based SERS, *Analyst*, vol. 138, no. 4, pp. 1020-1025, 2013.  
<https://doi.org/10.1039/C2AN36116G>
- [12] S. M. Yang, S. G. Jang, D. G. Choi, S. Kim, and H. K. Yu, Nanomachining by colloidal lithography, *Small*, vol. 2, no. 4, pp. 458-475, 2006.  
<https://doi.org/10.1002/sml.200500390>
- [13] X. Liang, R. Dong, and J. C. Ho, Self-assembly of colloidal spheres toward fabrication of hierarchical and periodic nanostructures for technological applications, *Adv. Mater. Technol.*, 2019, Art. no. 1800541.  
<https://doi.org/10.1002/admt.201800541>
- [14] D. Liu, W. Cai, M. Marin, Y. Yin, and Y. Li, Air-liquid interfacial self-assembly of two-dimensional periodic nanostructured arrays, *ChemNanoMat*, vol. 5, no. 11, pp. 1338-1360, 2019.  
<https://doi.org/10.1002/cnma.201900322>
- [15] N. V. Minh, N. T. Hue, N. T. H. Lien, and C. M. Hoang, Close-packed monolayer self-assembly of silica nanospheres assisted by infrared irradiation, *Electron. Mater. Lett.*, vol. 14, pp. 64-69, 2018.  
<https://doi.org/10.1007/s13391-017-6389-x>
- [16] N. V. Minh, N. N. Son, N. T. H. Lien, and C. M. Hoang, Non-close packaged monolayer of silica nanoparticles on silicon substrate using HF vapor etching, *Micro Nano Lett.*, vol. 17, pp. 1-4, 2017.  
<https://doi.org/10.1049/mnl.2016.0825>
- [17] W. Stober, A. Fink and E. Bohn, Controlled growth of monodisperse silica spheres in the micron size range, *J. Colloid Interface Sci*, vol. 26, no. 1, pp. 62-69, 1968.  
[https://doi.org/10.1016/0021-9797\(68\)90272-5](https://doi.org/10.1016/0021-9797(68)90272-5)
- [18] T. H. L. Nghiem, T. N. Le, T. H. Do, T. T. Duong, V. Q. Hoa, and D. H. N. Tran, Preparation and characterization of silica-gold core-shell nanoparticles, *J. Nanopart. Res.*, vol. 15, no. 11, pp. 1-9, 2013, Art. no. 2091.  
<https://doi.org/10.1007/s11051-013-2091-6>
- [19] E. Smith and G. Dent, *Modern Raman Spectroscopy: A Practical Approach*, John Wiley & Sons, Inc., 2005, pp. 123-128.  
<https://doi.org/10.1002/0470011831>
- [20] M. Moskovits, Surface-enhanced raman spectroscopy: a brief perspective, surface-enhanced raman scattering-physics and applications, *Topics Appl. Phys.*, 2006, 1-18.  
[https://doi.org/10.1007/3-540-33567-6\\_1](https://doi.org/10.1007/3-540-33567-6_1)
- [21] M. Alshehab, Design and construction of a raman microscope for nano-plasmonic structures, M.S. thesis, University of Ottawa, 2018.
- [22] C. Li, Y. Huang, K. Lai, B. A. Rasco, and Y. Fan, Analysis of trace methylene blue in fish muscles using ultra-sensitive surface-enhanced Raman spectroscopy, *Food control*, vol. 65, pp. 99-105, Jul. 2016.  
<https://doi.org/10.1016/j.foodcont.2016.01.017>
- [23] E. C. Le Ru, E. Blackie, M. Meyer, and P. G. Etchegoin, surface enhanced raman scattering enhancement factors: a comprehensive study, *J. Phys. Chem. C*, vol. 111, no. 37, pp. 13794-13803, 2007.  
<https://doi.org/10.1021/jp0687908>